AIP | Applied Physics Letters

Effect of rare earth metal on the spin-orbit torque in magnetic heterostructures

Kohei Ueda, Chi-Feng Pai, Aik Jun Tan, Maxwell Mann, and Geoffrey S. D. Beach

Citation: Applied Physics Letters **108**, 232405 (2016); doi: 10.1063/1.4953348
View online: http://dx.doi.org/10.1063/1.4953348
View Table of Contents: http://scitation.aip.org/content/aip/journal/apl/108/23?ver=pdfcov
Published by the AIP Publishing

Effect of rare earth metal on the spin-orbit torque in magnetic heterostructures

Kohei Ueda, Chi-Feng Pai, Aik Jun Tan, Maxwell Mann, and Geoffrey S. D. Beach[a)]
Department of Materials Science and Engineering, Massachusetts Institute of Technology, Cambridge, Massachusetts 02139, USA

(Received 3 March 2016; accepted 21 May 2016; published online 7 June 2016)

We report the effect of the rare earth metal Gd on current-induced spin-orbit torques (SOTs) in perpendicularly magnetized Pt/Co/Gd heterostructures, characterized using harmonic measurements and spin-torque ferromagnetic resonance (ST-FMR). By varying the Gd metal layer thickness from 0 nm to 8 nm, harmonic measurements reveal a significant enhancement of the effective fields generated from the Slonczewski-like and field-like torques. ST-FMR measurements confirm an enhanced effective spin Hall angle and show a corresponding increase in the magnetic damping constant with increasing Gd thickness. These results suggest that Gd plays an active role in generating SOTs in these heterostructures. Our finding may lead to spin-orbitronics device application such as non-volatile magnetic random access memory, based on rare earth metals. *Published by AIP Publishing.* [http://dx.doi.org/10.1063/1.4953348]

Current-driven magnetization switching[1–7] and magnetic domain wall motion[8–19] have been widely investigated for device applications such as nonvolatile magnetic memory.[9,20] More recently, current-induced control of the magnetization has been achieved by current-induced spin-orbit torques (SOTs) originating from heavy metal layers with strong spin-orbit coupling, from which the resulting effective fields are strong enough to control the magnetization in adjacent ultra-thin ferromagnetic layers.[1–7,11,13–19,21–35] In the ferromagnet/heavy metal system, SOTs can arise from the interfacial Rashba effect[11,21,24] and the bulk spin Hall effect (SHE),[2–4,7,13,16,22,23,27,29–35] and can produce both a Slonczewski-like (SL)[36] and field-like (FL) torque.[37] The SL torque, which manifests predominantly from the SHE, has an anti-damping form and is responsible for magnetic switching and current-driven domain wall motion. Therefore, substantial efforts have been made both to clarify the origins of this torque and to identify materials that can enhance it in magnetic heterostructures for device applications.

In order to characterize the sign and magnitude of SOTs, the corresponding effective fields from the SL-torque (H_{SL}) and FL-torque (H_{FL}) are commonly measured using techniques such as harmonic voltage measurements[21,25,28] and spin torque-ferromagnetic resonance (ST-FMR).[22] Under the assumption that H_{SL} derives solely from the SHE, the effective spin Hall angle θ_{SH} that gives the ratio of spin current to in-plane charge current serves as a convenient figure of merit to characterize the strength of the SL-torque. Pt, Ta, and W have been the most widely investigated spin Hall metals due to their relatively high spin Hall angles, θ_{SH} ($\sim+0.07$ for Pt,[3,13,22,31,33] ~-0.15 for β−Ta,[2] and ~-0.30 for β-W[4]). By sandwiching ultra-thin Co between Pt and Ta, which show opposite signs of θ_{SH}, an enhancement of the effective θ_{SH} up to 0.34 was achieved due to the contribution from both spin Hall metals.[29] To date, investigations of SOTs have mainly focused on transition heavy metals such as Pt,[3,13,22,23,31–34] Ta,[2,25,35] W,[4] Hf,[7,27] etc., on their thickness dependence,[7,16,25,27] on the effect of different oxide cap layers,[30] and on different ferromagnetic layers such as Co and CoFeB.[7,32,33] For exploring new spin Hall materials, the rare earth (RE) metals are expected to be a potential SOT source because of the strong spin-orbit coupling[38] in these materials. However, to date, there have been no studies of SOTs originating from ferromagnet/RE interfaces.

In this letter, we examine SOTs generated by a Co/Gd interface in Pt/Co/Gd heterostructures. Films with in-plane magnetized Co and ultra-thin Co with perpendicular magnetic anisotropy (PMA) were prepared for ST-FMR and harmonic measurements, respectively. The SOTs were characterized as a function of Gd layer thickness t_{Gd}. In these heterostructures, if the Gd layer would produce SOT, then the resulting effective fields will be greater or lower than those from a Pt/Co bi-layer structure, which allows the contribution from the Co/Gd interface to be inferred. Interestingly, we find that both the SL and FL SOTs are significantly enhanced by increasing t_{Gd}, suggesting that Gd acts as an effective SOT source.

First, we performed harmonic measurements to estimate the SOT efficiency. We prepared a series of substrate/Ta (4 nm)/Pt (3 nm)/Co (0.9 nm)/Gd (t_{Gd}) structures capped by 3 nm Ta using d.c. magnetron sputtering onto thermally oxidized Si substrates, as shown schematically in Fig. 1(a). t_{Gd} was varied from 2 nm to 8 nm. The Ta capping layer prevents oxidation of the Gd layer, while the bottom Ta layer serves as seed layer. Pt was used as an underlayer to generate PMA in the Co layer. The deposition was performed at room temperature under 3 mTorr Ar with a base pressure of 3×10^{-7} Torr. Similarly prepared Gd films capped with Ta exhibited a resistivity $\rho_{Gd} = 525.0\ \mu\Omega\,\text{cm}$, which is somewhat higher but reasonably consistent with prior measurements[39] of nanocrystalline Gd, indicating minimal oxidation of the Gd metal.

A control sample with $t_{Gd} = 0$ was also fabricated, with the structure substrate/Ta(4 nm)/Pt(3 nm)/Co(0.9 nm)/GdOx(3 nm), where the GdOx layer was grown by reactive sputtering of a

a)Author to whom correspondence should be addressed. Electronic mail: gbeach@mit.edu

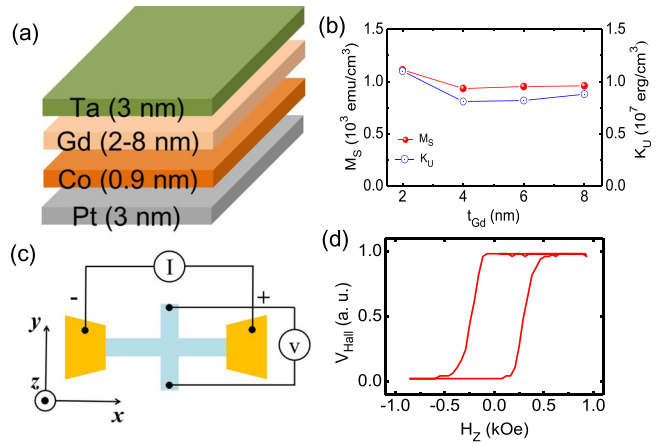

FIG. 1. (a) Schematic illustration of Pt/Co/Gd heterostructures. (b) Saturation magnetization (M_S) and perpendicular magnetic anisotropy energy density (K_U) versus Gd layer thickness t_{Gd}. (c) Illustration of a patterned device with conventional harmonic measurement set-up and coordinate system. (d) Hall measurement under H_Z in a film with $t_{Gd} = 6$ nm.

Gd metal target with an oxygen partial pressure of ~0.1 mTorr. Here, GdOx served as the capping layer rather than Ta, since Ta in contact with Co is known to enhance the SOT in Pt/Co/Ta heterostructures.[29]

To estimate magnetic properties such as saturation magnetization (M_S) and PMA energy density (K_U) in the films, we obtained out-of-plane and in-plane hysteresis loops using a vibrating sample magnetometer (VSM). Here, K_U is given by $K_U = M_S H_K/2$ with $H_K = H_{sat} + 4\pi M_S$, where H_K is the magnetic anisotropy field and H_{sat} is the hard-axis saturation field. All films showed PMA, which is known to be driven by the Pt/Co interface.[40] As summarized in Fig. 1(b), M_S and K_U are both almost constant with respect to t_{Gd}, suggesting that Gd is not a critical factor in achieving PMA and its thickness variation does not change the magnetic properties of the Co.

Next, we performed harmonic voltage measurements by detecting Hall voltage variations as a function of magnetization tilting under in-plane magnetic fields to quantify the SOTs.[21,25] For these measurements, Hall bar devices with lateral dimensions 5 μm-width and 12 μm-length were patterned by photolithography and lift off after sputter deposition (Fig. 1(c)). Ta (5 nm)/Au (50 nm) pads were attached to the ends of the Hall bar arms to inject a.c. current with low frequency and to detect the Hall voltage (V_{Hall}). As shown in Fig. 1(c), the coordinate axes z, x, and y correspond, respectively, to the direction perpendicular to the film, in-plane along the current-flow direction, and transverse to the current in the film plane. Fig. 1(d) shows a typical Hall voltage measurement versus out-of-plane field H_Z for $t_{Gd} = 6$ nm, under low a.c. current density (2×10^{10} A/m^2). The high coercivity and remanence of this out-of-plane hysteresis loop shows that patterning does not compromise the PMA of the films.

Harmonic SOT measurements were carried out as follows. An a.c. current I was driven along the x-direction (Fig. 1(c)) by applying an a.c. voltage with rms amplitude V_{in} and frequency $\omega/2\pi = 1.77$ kHz. The first and second harmonics ($V_{1\omega}$ and $V_{2\omega}$, respectively) of the Hall voltage were measured using a lock-in amplifier. $V_{1\omega}$ and $V_{2\omega}$ were recorded as a function of applied in-plane field H_x (H_y), as shown in Fig. 2. Then, H_{SL} and H_{FL} were estimated using the relation[25]

$$H_{SL(FL)} = \frac{-2\left(\frac{dV_{2\omega}}{dH_{x(y)}}\right)}{\left(\frac{d^2V_{1\omega}}{dH_{x(y)}^2}\right)}. \quad (1)$$

Figures 2(a) and 2(b) show $V_{1\omega}$ and $V_{2\omega}$ versus H_x for $t_{Gd} = 6$ nm, measured with the out-of-plane magnetization component $M_Z > 0$ and with $M_Z < 0$. Figures 2(c) and 2 (d) show the corresponding results for H_y. $V_{2\omega}$ varies linearly with both H_x and H_y, with a slope that is the same for H_x and reversed for H_y when M_z is reversed, as expected from the contributions of H_{SL} and H_{FL}.[13,16,25,29,33]

Figures 3(a) and 3(b) show the estimated H_{SL} and H_{FL} using Eq. (1) as a function of V_{In} for various t_{Gd}. The effective

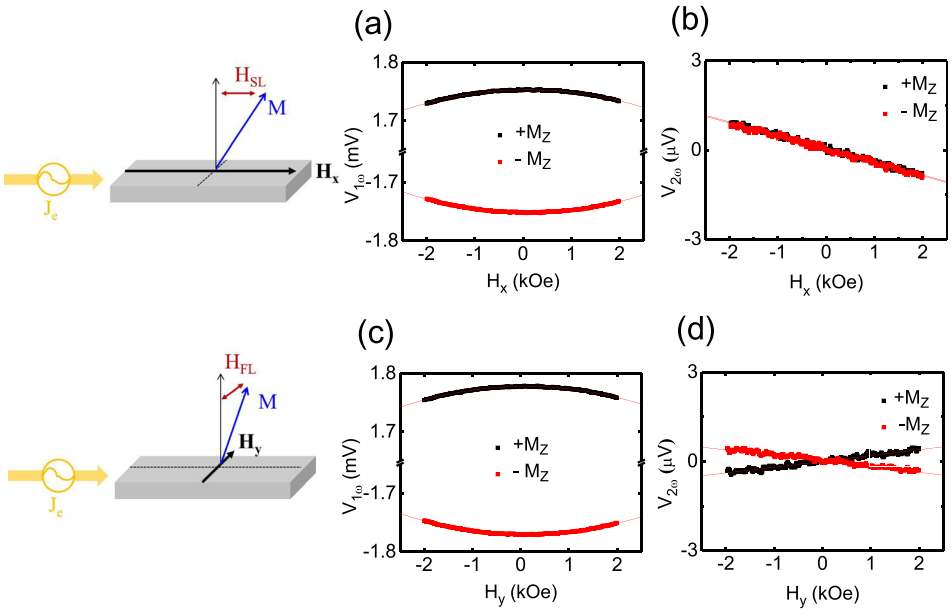

FIG. 2. (a) First-harmonic signal $V_{1\omega}$ and (b) second-harmonic signal $V_{2\omega}$ versus H_x. (c) $V_{1\omega}$ and (d) $V_{2\omega}$ under H_y. Measurement geometries are shown schematically to the left of the corresponding plots. Note that a sample-dependent offset voltage has been subtracted from the harmonic data.

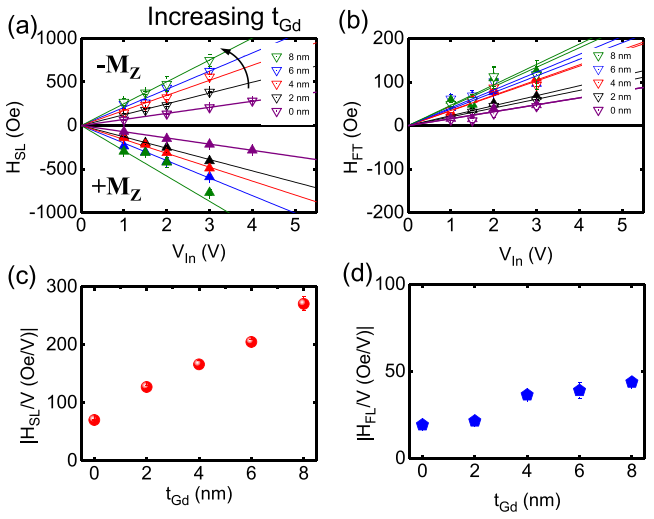

FIG. 3. (a) Effective field H_{SL} and (b) H_{FL} as a function ac input voltage for various Gd layer thicknesses t_{Gd}. (c), (d) Absolute value of effective fields per unit ac input voltage, $|H_{SL(FL)}/V_{In}|$ as a function of t_{Gd}.

fields vary linearly with V_{In}, indicating that the effects of Joule heating are negligible in the measured V_{In} range. We find that the sign of H_{SL} depends on the direction of M_Z, while that of H_{FL} is independent of M_Z. This result is consistent with previous reports using the same method.[13,16,33]

Figure 3(c) shows H_{SL} per unit applied voltage ($|H_{SL}/V_{In}|$) as a function of t_{Gd}, obtained from the fitted slope of H_{SL} versus V_{In} in Fig. 3(a). The $|H_{SL}/V_{In}|$ indicates absolute values, estimated from an average value of absolute efficiencies for $+M_Z$ and $-M_Z$. Interestingly, $|H_{SL}/V_{In}|$ significantly increases with increasing Gd thickness, increasing from 70 Oe/V for the sample with $t_{Gd} = 0$ to ~270 Oe/V when $t_{Gd} = 8$ nm. We note that here it is more convenient to compare H_{SL} per unit applied voltage rather than per unit current density, as this avoids ambiguities due to the variation of the current distribution in the heterostructure as the Gd layer thickness is varied. That is to say, assuming that the Pt, Co, and Gd layers act as parallel resistance paths, the current flowing in the Pt layer and hence the SOT generated by the Pt layer, at a given V_{In}, will be invariant with t_{Gd}, since the resistance of the Pt layer is independent of t_{Gd}. Therefore, since $|H_{SL}/V_{In}|$ increases with t_{Gd}, we can infer that the Gd metal at the top interface produces SL-SOT acting on the magnetic moment in Co layer since the SOT per unit drive voltage contributed by the Pt layer is the same for this set of samples independent of t_{Gd}. Furthermore, the enhancement of $|H_{SL}/V_{In}|$ suggests that Gd has an opposite sign of θ_{SH} compare to that of Pt, so that the SL-SOTs generated at the top and bottom interfaces are additive.

In Fig. 3(d), we plot H_{FL} per unit voltage, $|H_{FL}/V_{In}|$, as a function of t_{Gd}. With increasing t_{Gd}, the field-like torque increases systematically by about a factor of 2, indicating that Gd can also enhance the FL-SOT. However, the relative strength of H_{SL} is in all cases much larger than H_{FL}, suggesting that the SHE is the dominant SOT mechanism.

Although a large SOT contribution from Gd is obtained, an accurate estimation of the spin Hall angle θ_{SH} is difficult due to the complicated current distribution, as is generally the case when quantitatively assessing SOTs in heterostructures. To estimate the current distribution in the stack, we measured the resistivity ρ for each layer by preparing single-layer films, yielding $\rho_{Pt} = 31.9\ \mu\Omega\,\text{cm}$, $\rho_{Co} = 65.6\ \mu\Omega\,\text{cm}$, $\rho_{Gd} = 525.0\ \mu\Omega\,\text{cm}$, and $\rho_{Ta} = 372.8\ \mu\Omega\,\text{cm}$. By comparing these resistivities, we expect that the Pt layer will shunt most of the current. By normalizing the effective field to the current density flowing in the Pt layer, we arrive at an effective spin Hall angle θ_{SH}^{eff}, which ranges from 0.20 ±0.02 to 0.78±0.02 as t_{Gd} is increased. The inferred θ_{SH}^{eff} for $t_{Gd} = 0$ is somewhat larger than that typically found for Pt, which may be attributed to uncertainties in current distribution and differences in transparency at the Co/Pt interface, which depends sensitively on the details of the interface and directly impacts the spin-mixing conductance[32,33] and hence θ_{SH}^{eff}. The significant relative increase of θ_{SH}^{eff} with increasing t_{Gd} clearly indicates that the Co/Gd interface is contributing additional SL-SOT.

To confirm the presence of additional SOT from Gd metal, we conducted ST-FMR measurements, which are widely used to determine the efficiencies of SOTs.[2,4,7,22,23,31–33,35] The measurement provides important magnetic parameters such as demagnetization ($4\pi M_{eff}$), the damping constant (α) and θ_{SH}. We prepared samples with the structure substrate/Gd (t)/Co (5 nm)/Pt (4 nm) with in-plane anisotropy by dc magnetron sputtering. t_{Gd} was varied 0 to 8 nm with 2 nm steps. Devices with lateral dimensions of 10 μm × 10 μm with Ta (5 nm)/Au (50 nm) electrode pads, were patterned by photolithography and lift-off in the same manner as were the devices for harmonic measurements. Fig. 4(a) shows a schematic illustration of the sample measurement configuration. Measurements were performed by sweeping an in-plane magnetic field in the range −3 kOe to +3 kOe with various RF injection power frequencies (f) at room temperature. The dc output mixing voltage (V_{mix}) of the ST-FMR spectra, which consists of symmetric and antisymmetric components, was measured using a lock-in amplifier.

Figures 4(b) and 4(c) show typical ST-FMR spectra for Co/Pt and Gd/Co/Pt at 9 GHz. The spectra in the positive field range were fitted by a sum of symmetric and antisymmetric

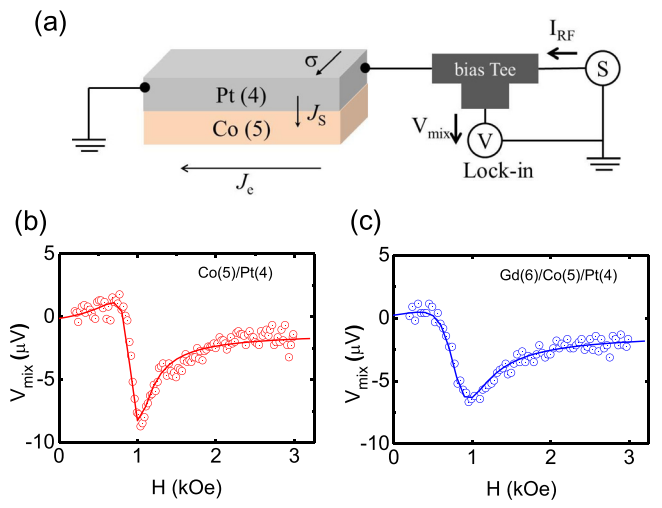

FIG. 4. (a) Schematic illustration of ST-FMR measurement. Signal generator applies a.c. current exciting FMR in Co layer and generating SHE in Pt layer. J_S and σ indicate directions of induced spin current flow and spin current polarization, respectively. (b), (c) typical ST-FMR spectra with fits for (b) Co/Pt and for (c) Gd(6)/Co/Pt at 9 GHz.

Lorentzian functions[2,4,7,22,23,31–33,35] to yield the resonance field (H_0) and the line width (Δ). Figure 5(a) shows typical results of f versus H_0 for Co/Pt and Gd (6 nm)/Co/Pt samples fitted by the Kittel fomula, $f = \frac{2\pi}{\gamma}\sqrt{H_0(H_0 + 4\pi M_{eff})}$, where γ is the gyromagnetic ratio. Extracted $4\pi M_{\text{eff}}$ are estimated to be 10.13 ± 0.02 kOe for Co/Pt and 11.12 ± 0.07 kOe for Gd/Co/Pt. These values agree well with the hard axis saturation field measured in continuous films by VSM. Figure 5(b) shows Δ versus f together with a linear fit using $\Delta = \frac{2\pi f}{\gamma}\alpha$, where α is the damping constant. From the slopes, we obtained $\alpha_{\text{Co/Pt}} = 0.025 \pm 0.006$ and $\alpha_{\text{Gd(6)/Co/Pt}} = 0.043 \pm 0.003$.

Next, we estimated θ_{SH}, using the expression[22] $\theta_{SH} = \frac{S}{A}\left(\frac{e}{\hbar}\right)4\pi M_S t_{FM} d_{HM}\sqrt{1 + \left(\frac{4\pi M_{\text{eff}}}{H_0}\right)}$. Here, S/A is the amplitude ratio of symmetric (S) and antisymmetric (A) components of the ST-FMR spectra, e is the charge electron, $\hbar$ is the Planck constant, t_{FM} is the thickness of ferromagnetic layer, and d_{HM} is the thickness of heavy metal layer. S and A are given by $\frac{\hbar}{2e}\frac{J_{\text{rf}}}{4\pi M_S t_{\text{FM}}}$ and $\frac{J_{\text{rf}} d_{\text{HM}}}{2}\sqrt{1 + \left(\frac{4\pi M_{\text{eff}}}{H_0}\right)}$, respectively, where J_{rf} is the rf charge current density in HM layer.

θ_{SH} and α are plotted as a function of t_{Gd} in Figs. 5(c) and 5(d). Individual data points represent an average of measurement results on five separate devices, and error bars represent the standard deviation. We found that θ_{SH} increases with increasing t_{Gd}, ranging from ~0.06 to ~0.10 as t_{Gd} is increased to 6 nm, and then seems to plateau, although more data are required in the high thickness regime to confirm this latter behavior. The minimum value at $t_{\text{Gd}} = 0$ nm comes from the SOT contribution of only Pt and is in good agreement with previous studies.[22,31,33] The data are qualitatively, but not quantitatively, consistent with the harmonic measurement results performed on samples with thinner ferromagnetic layers as described above. This could reflect differences in spin transmission for PMA versus in-plane magnetized samples. In addition, one can expect differences in current-flow distributions and spin transmission due to the fact that the top interface is very close to the bottom interface in the PMA samples, which could complicate the scattering mechanisms, whereas the two interfaces are far from one another in the thicker in-plane samples used for ST-FMR. However, the qualitative agreement between the two measurements, indicating that the effective θ_{SH} increases with increasing t_{Gd}, suggests that the Gd layer is indeed contributing significantly to the net SOT.

To further understand this enhanced θ_{SH}, we focus on the t_{Gd} dependence on α, shown in Fig. 5(d). Interestingly, α also increases with increasing t_{Gd}, varying from 0.025 ± 0.004 to 0.045 ± 0.004 in this set of samples. The measured damping for $t_{\text{Gd}} = 0$ nm with a Co thickness of 5 nm agrees well with the results reported by Pai *et al.*[33] The correlation between θ_{SH} and α, which both increase with increasing t_{Gd}, could suggest that enhanced interface scattering mechanisms are related to the increased SOT that we observe.

Finally, in order to directly examine the effect of Gd metal, we attempted measuring Gd/Co bi-layer films without the Pt overlayer. The film structure used was substrate/Gd(t)/Co(5 nm)/GdOx(5 nm), where t_{Gd} is varied in the range from 2 to 20 nm. However, the ST-FMR signal-to-noise was insufficient to extract meaningful parameters, which we attribute to the low injected power due to the high resistivity of films.

In conclusion, we have investigated the effect of Gd metal on SOT in Pt/Co/Gd heterostructures with PMA and in-plane anisotropy, using conventional harmonic and ST-FMR measurements, respectively. We find an enhancement of the SOT with increasing Gd metal layer thickness, as characterized by the effective fields H_{SL} and H_{FL}. ST-FMR measurement also reveals enhanced effective θ_{SH} and α in films with thicker Gd, suggesting a correlation between damping and SOT enhancement at the Co/Gd interface. These results indicate that the rare-earth metal Gd can be used to significantly enhance SOTs in thin-film heterostructures.

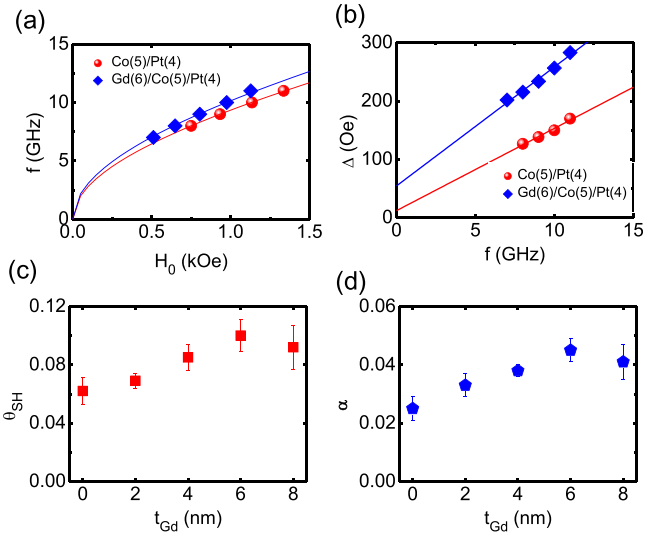

FIG. 5. (a) Frequency (f) as a function of resonance field. (b) Line width (Δ) as a function of f. (c) Spin Hall angle and (d) magnetic damping constant as function of Gd thickness.

This work was supported by the National Science Foundation under NSF-ECCS-1408172 and by the Samsung Global MRAM Innovation Program.

[1]M. Miron, K. Garello, G. Gaudin, P.-J. Zermatten, M. V. Costache, S. Auffret, S. Bandiera, B. Rodmacq, A. Schuhl, and P. Gambardella, Nature **476**, 189 (2011).
[2]L. Liu, C.-F. Pai, Y. Li, H. W. Tseng, D. C. Ralph, and R. A. Buhrman, Science **336**, 555 (2012).
[3]L. Liu, O. J. Lee, T. J. Gudmundsen, D. C. Ralph, and R. A. Buhrman, Phys. Rev. Lett. **109**, 096602 (2012).
[4]C.-F. Pai, L. Liu, Y. Li, H. W. Tseng, D. C. Ralph, and R. A. Buhrman, Appl. Phys. Lett. **101**, 122404 (2012).
[5]K. Garello, C.-O. Avci, I.-M. Miron, M. Baumgartner, A. Ghosh, S. Auffret, O. Boulle, G. Gaudin, and P. Gambardella, Appl. Phys. Lett. **105**, 212402 (2014).
[6]J. Torrejon, F. Garcia-Sanchez, T. Taniguchi, J. Sinha, S. Mitani, J.-V. Kim, and M. Hayashi, Phys. Rev. B **91**, 214434 (2015).
[7]M.-H. Nguyen, C.-F. Pai, K. X. Nguyen, D. A. Muller, D. C. Ralph, and R. A. Buhrman, Appl. Phys. Lett. **106**, 222402 (2015).
[8]A. Yamaguchi, T. Ono, S. Nasu, K. Miyake, K. Mibu, and T. Shinjo, Phys. Rev. Lett. **92**, 077205 (2004).
[9]S. S. P. Parkin, M. Hayashi, and L. Thomas, Science **320**, 190 (2008).
[10]T. Koyama, D. Chiba, K. Ueda, K. Kondou, H. Tanigawa, S. Fukami, T. Suzuki, N. Ohshima, N. Ishiwata, Y. Nakatani, K. Kobayashi, and T. Ono, Nat. Mater. **10**, 194 (2011).
[11]I. M. Miron, T. Moore, H. Szambolics, L. D. Buda-Prejbeanu, S. Auffret, B. Rodmacq, S. Pizzini, J. Vogel, M. Bonfim, A. Schuhl, and G. Gaudin, Nat. Mater. **10**, 419 (2011).

[12]K. Ueda, T. Koyama, R. Hiramatsu, D. Chiba, S. Fukami, H. Tanigawa, T. Suzuki, N. Ohshima, N. Ishiwata, Y. Nakatani, K. Kobayashi, and T. Ono, Appl. Phys. Lett. **100**, 202407 (2012).
[13]S. Emori, U. Bauer, S. M. Ahn, E. Martinez, and G. S. D. Beach, Nat. Mater. **12**, 611 (2013).
[14]K.-S. Ryu, L. Thomas, S.-H. Yang, and S. S. P. Parkin, Nat. Nanotechnol. **8**, 527 (2013).
[15]K.-S. Ryu, S.-H. Yang, L. Thomas, and S. S. P. Parkin, Nat. Commun. **5**, 3910 (2014).
[16]J. Torrejon, J. Kim, J. Sinha, S. Mitani, M. Hayashi, M. Yamanouchi, and H. Ohno, Nat. Commun. **5**, 4655 (2014).
[17]K. Ueda, K. J. Kim, Y. Yoshimura, R. Hiramatsu, T. Moriyama, D. Chiba, H. Tanigawa, T. Suzuki, E. Kariyada, and T. Ono, Appl. Phys. Express **7**, 053006 (2014).
[18]D. Bang and H. Awano, J. Appl. Phys. **117**, 17D916 (2015).
[19]K. Ueda, K.-J. Kim, T. Taniguchi, T. Tono, T. Moriyama, and T. Ono, Phys. Rev. B **91**, 060405(R) (2015).
[20]A. Fert, V. Cros, and J. Sampaio, Nat. Nanotechnol. **8**, 152 (2013).
[21]U. H. Pi, K. W. Kim, J. Y. Bae, S. C. Lee, Y. J. Cho, K. S. Kim, and S. Seo, Appl. Phys. Lett. **97**, 162507 (2010).
[22]L. Liu, T. Moriyama, D. C. Ralph, and R. A. Buhrman, Phys. Rev. Lett. **106**, 036601 (2011).
[23]K. Kondou, H. Sukagawa, S. Mitani, K. Tsukagoshi, and S. Kasai, Appl. Phys. Express **5**, 073002 (2012).
[24]K.-W. Kim, S.-M. Seo, J. Ryu, K.-J. Lee, and H.-W. Lee, Phys. Rev. B **85**, 180404 (2012).
[25]J. Kim, J. Sinha, M. Hayashi, M. Yamanouchi, S. Fukami, T. Suzuki, S. Mitani, and H. Ohno, Nat. Mater. **12**, 240 (2013).
[26]J. Kim, J. Sinha, S. Mitani, M. Hayashi, S. Takahashi, S. Maekawa, M. Yamanouchi, and H. Ohno, Phys. Rev. B **89**, 174424 (2014).
[27]C.-F. Pai, M.-H. Nguyen, C. Belvin, L. H. Vilela-Leão, D. C. Ralph, and R. A. Buhrman, Appl. Phys. Lett. **104**, 082407 (2014).
[28]K. Garello, I. M. Miron, C. O. Avci, F. Freimuth, Y. Mokrousov, S. Blügel, S. Auffret, O. Boulle, G. Gaudin, and P. Gambardella, Nat. Nanotechnol. **8**, 587 (2013).
[29]S. Woo, M. Mann, A.-J. Tan, L. Caretta, and G. S. D. Beach, Appl. Phys. Lett. **105**, 212404 (2014).
[30]M. Akyol, J.-G. Alzate, G. Yu, P. Upadhyaya, K.-L. Wong, A. Ekicibil, P.-K. Amiri, and K.-L. Wang, Appl. Phys. Lett. **106**, 032406 (2015).
[31]T. Nan, S. Emori, C.-T. Boone, X. Wang, T.-M. Oxholm, J.-G. Jones, B.-M. Howe, G.-J. Brown, and N.-X. Sun, Phys. Rev. B **91**, 214416 (2015).
[32]W. Zhang, W. Han, X. Jiang, S.-H. Yang, and S. S. P. Parkin, Nat. Phys. **11**, 496 (2015).
[33]C.-F. Pai, Y. Ou, L. H. Viela-Leao, D. C. Ralph, and R. A. Buhrman, Phys. Rev. B **92**, 064426 (2015).
[34]K.-F. Huang, D.-S. Wang, H.-H. Lin, and C.-H. Lai, Appl. Phys. Lett. **107**, 232407 (2015).
[35]K. Kondou, H. Sukegawa, S. Kasai, S. Mitani, Y. Niimi, and Y. Otani, Appl. Phys. Express **9**, 023002 (2016).
[36]J. C. Slonczewski, J. Magn. Magn. Mater. **159**, L1 (1996).
[37]S. Zhang, P. M. Levy, and A. Fert, Phys. Rev. Lett. **88**, 236601 (2002).
[38]R. Brout and H. Suhi, Phys. Rev. Lett. **2**, 387 (1959).
[39]H. Zeng, Y. Wu, J. Zhang, C. Kuang, M. Yue, and S. Zhao, Prog. Nat. Sci.: Mater. Int. **23**, 18 (2013).
[40]M. T. Johnson, P. J. H. Bloemenzx, F. J. A. den Broedery, and J. J. de Vriesz, Rep. Prog. Phys. **59**, 1409 (1996).